A Mechanism of Protein-Mediated Fusion: Coupling between Refolding of the Influenza Hemagglutinin and Lipid Rearrangements

Michael M. Kozlov* and Leonid V. Chernomordik#

*Department of Physiology and Pharmacology, Sackler Faculty of Medicine, Tel Aviv University, Ramat Aviv, Tel Aviv 69978, Israel, and #The Laboratory of Cellular and Molecular Biophysics, National Institute of Child Health and Human Development, National Institutes of Health, Bethesda, Maryland 20892 USA

ABSTRACT Although membrane fusion mediated by influenza virus hemagglutinin (HA) is the best characterized example of ubiquitous protein-mediated fusion, it is still not known how the low-pH-induced refolding of HA trimers causes fusion. This refolding involves 1) repositioning of the hydrophobic N-terminal sequence of the HA2 subunit of HA ("fusion peptide"), and 2) the recruitment of additional residues to the α-helical coiled coil of a rigid central rod of the trimer. We propose here a mechanism by which these conformational changes can cause local bending of the viral membrane, priming it for fusion. In this model fusion is triggered by incorporation of fusion peptides into viral membrane. Refolding of a central rod exerts forces that pull the fusion peptides, tending to bend the membrane around HA trimer into a saddle-like shape. Elastic energy drives self-assembly of these HA-containing membrane elements in the plane of the membrane into a ring-like cluster. Bulging of the viral membrane within such cluster yields a dimple growing toward the bound target membrane. Bending stresses in the lipidic top of the dimple facilitate membrane fusion. We analyze the energetics of this proposed sequence of membrane rearrangements, and demonstrate that this simple mechanism may explain some of the known phenomenological features of fusion.

INTRODUCTION

Fusion of two membranes into one is a common stage in diverse cell biological processes. Entry of numerous pathogenic viruses into their host cells is dependent on the fusion of the viral envelope with cell membranes (Hernandez et al., 1996). Although the localization, timing, and rates of biological fusion are tightly regulated by specialized "fusion" proteins (Pevsner and Scheller, 1994), ultimately it is two membrane lipid bilayers that must merge in fusion.

Protein-mediated fusion of biological membranes shares a number of important features with fusion of protein-free lipid bilayers:

Biological fusion and lipid bilayer fusion similarly depend on the lipid composition of the outer and inner monolayers of interacting membranes (see, for review, Chernomordik et al., 1995b, 1997, 1998).

Hemifusion, an early stage of lipid bilayer fusion (Chernomordik et al., 1995a, 1998; Chenturiya et al., 1997; Lee and Lentz, 1997), was recently documented for protein-mediated fusion (Kemble et al., 1994; Melikyan et al., 1995). At this stage the contacting monolayers of the membranes merge, whereas the inner (distal) monolayers and aqueous contents of cells or lipid bilayers remain distinct.

Finally, early fusion pores (i.e., aqueous junctions between membrane contents) have similar characteristics for biological fusion and fusion of lipid bilayers (Monck and Fernandez, 1992; Nanavati et al., 1992; Chanturiya et al., 1997; Lee and Lentz, 1997; Melikyan and Chernomordik, 1997; Chernomordik et al., 1998).

These findings suggest that biological fusion, like lipid bilayer fusion (see, for review, Chernomordik et al., 1995b; Siegel and Epand, 1997), involves the formation of transient and local nonbilayer fusion intermediates characterized by strong bending of membrane monolayers. However, it is still not known how fusion proteins catalyze these membrane rearrangements and fuse lipid bilayers that would not fuse on their own (Stegmann, 1993; Alford et al., 1994).

The best characterized fusion protein, influenza virus hemagglutinin (HA), is a homotrimeric envelope glycoprotein (Wiley and Skehel, 1987; White, 1996). Each HA monomer consists of two subunits: HA1, responsible for virus attachment to sialic acid-containing viral receptor of target membranes, and membrane-bound HA2, responsible for fusion.

Fusion reaction is associated with two main transformations of the state of HA molecules.

First, each HA trimer participating in fusion undergoes refolding to a new, fusion-competent conformation. This process, also referred to as low-pH-activation of HA, is triggered by acidic environment in endosomes (White, 1996). The important feature of this refolding is the change in position of the conserved, hydrophobic amino-terminal peptide of HA2 (fusion peptide). In the initial conformation of HA the fusion peptide is hidden within the center of the trimeric stem at a distance of 3.5 nm from the viral membrane and 10 nm from the target membrane (Wiley and Skehel, 1987). During refolding, the fusion peptide is exposed and inserts into both viral and target membranes (see, for review, Gaudin et al., 1995). In the final, low-pH form

Received for publication 9 December 1997 and in final form 21 May 1998.

Address reprint requests to Dr. Michael M. Kozlov, Department of Physiology and Pharmacology, Sackler Faculty of Medicine, Tel Aviv University, Ramat Aviv, Tel Aviv 69978, Israel. Tel.: 972-3-640-7863; Fax: 972-3-640-9113; E-mail: misha@devil.tav.ac.il.

0006-3495/98/09/1384/13 $2.00

of the HA trimer, recruitment of additional residues to the triple-stranded α-helical coiled coil (Bullough et al., 1994; Carr and Kim, 1993) results in the formation of a rigid rod $\sim$10 nm in length (Bullough et al., 1994).

Second, fusion is a cooperative event that requires multiple (three to six) HA trimers (Blumenthal et al., 1996; Danieli et al., 1996). It is thought that low-pH-activated trimers self-assemble to form ring-like clusters surrounding future fusion sites (Bentz et al., 1990; Blumenthal et al., 1995; Danieli et al., 1996; Zimmerberg et al., 1993). Within this ring, membranes in the site of merger can be depleted from proteins, as suggested by similarities between HA-mediated fusion and the fusion of purely lipid bilayers (Chernomordik et al., 1997).

An existing hypothesis on the role of HA in triggering membrane fusion suggests that after low-pH activation, the fusion peptide first moves to the end of the α-helical coiled-coil rod directed toward the target membrane, and then binds to this membrane (Bullough et al., 1994; Weissenhorn et al., 1997). Subsequent development of the outer helical layer on the outside of the central coiled-coil of HA2 pulls together target membrane with an inserted fusion peptide and viral membrane with the transmembrane anchor of HA2 (Hernandez et al., 1996). An alternative hypothesis suggests that the attachment of the fusion peptide to the target membrane in a fusion-competent HA conformation is mediated by tilting the HA trimer (Stegmann et al., 1990; Guy et al., 1992; Tatulian et al., 1995), rather than by its major refolding. It was also suggested that after initial binding of the fusion peptide to the target membrane, the coiled coil of HA splays apart and "melts" into the target membrane, bringing it into contact with the viral membrane (Yu et al., 1994). In the "cast and retrieve" model (Zimmerberg et al., 1993), fusion peptide insertion into the target membrane triggers the transition of the peptide into α-helical conformation, which causes a significant decrease in its length. The contraction of the fusion peptides of adjacent HA trimers forces the target membrane first to dimple toward, and then to fuse with the viral membrane. In yet another model, fusion peptides exposed but not inserted into membranes dehydrate the intermembrane space in the fusion site and thus allow lipid merger (Bentz et al., 1990). In all of these models, insertion of the fusion peptide into the viral membrane has been assumed to correspond to an "inactivated" state that is unable to induce membrane fusion (Weber et al., 1994). Only in the model by Guy et al. (1992) is the interaction of the fusion peptides with the viral membrane considered to be a necessary step of the fusion process. In this model initial insertion of some fusion peptides into the viral membrane results in tilted orientation of HA trimers relative to the membrane, and gives rise to interaction of the remaining fusion peptides with the target membrane, the latter being followed by fusion.

All of these hypotheses, however, do not explain the origin of the driving forces for the self-assembly of HA and its role in the fusion mechanism. Furthermore, it gives no insight into the physical mechanisms by which either some specific low-pH conformation of HA or the transition between different conformations causes the rearrangements and fusion of membrane lipid bilayers.

In this study we propose a hypothetical mechanism of protein-mediated fusion of lipid bilayers that explains some of the established features of the HA-mediated fusion and suggests a new possible role for the fusion peptide. In contrast to most existing hypotheses, in our model, fusion is mediated by HA with fusion peptides inserted into viral membrane. In other words, we consider the conformation that is usually postulated to be inactive to be of primary significance for fusion.

We suggest that

A "spring" loaded between the stem of HA and its fusion peptide embedded into viral membrane produces a bending moment that tends to bend the membrane in the vicinity of the HA trimer, locally inducing a saddle-like shape of the membrane. The resulting complex of the trimer with the membrane will be called below the saddle-like membrane element.

To minimize the developed mechanical stress, saddle-like membrane elements self-assemble into a ring-like cluster, with a lipidic spot within the ring. The cluster induces bulging of the viral membrane and formation of a dimple with a lipidic top growing toward the target membrane.

This dimple brings the lipid bilayer of viral membrane close to the target membrane (provided that the membranes are kept together by HA1 interaction with sialic acids on the surface of the target membrane and by that of HA2 molecules that inserted their peptides into target membrane). Bending stresses in the lipidic top of the dimple facilitate its fusion with the target membrane.

MODEL

Because HA has the power to fuse lipid bilayers in the absence of any other proteins (Stegmann, 1993), in our analysis we will consider HA to be the only protein species present.

We assume that the ectodomain of low pH-activated HA at the time of fusion is a rigid structure capable of exerting the force. X-ray data suggest that the C-terminal fragment of the HA2 ectodomain located between coiled-coil and the transmembrane domain is disordered in the low pH conformation and, thus, can be rather flexible. This may lead to tilting of HA2 rods with respect to the membrane plane (Tatulian et al., 1995) or to stretching of the disordered C-terminal fragment along the rigid rod (Hughson, 1995). Electron microscopy data on the morphology of HA spikes for different strains of HA at low pH show no major changes in the appearance of these spikes on the time scale of membrane fusion (recently reviewed in Shangguan et al., 1997). These findings and the observation that the low pH form of HA2 also appears perpendicular to the membranes (Wharton et al., 1995) indicate that HA is not flexible enough to significantly bend and reorient along the plane of

the membrane. There is also no experimental evidence for stretch of the disordered C-terminal fragment.

We will also assume that membranes around the future fusion site are kept together at an average distance of 10 nm. Experimental data suggest that this binding is mediated by HA1 interaction with sialic acids on the surface of the target membrane (Wiley and Skehel, 1987), complemented, after low pH application, by insertion of fusion peptides of several HA trimers into target membrane (Schoch et al., 1992; Chernomordik et al., 1997). However, note that our model does not suggest or require any specific mechanism of the binding between membranes.

Saddle-like membrane element

Let us first consider one HA trimer embedded in a lipid bilayer. In the neutral pH conformation, each HA monomer is anchored in the viral membrane by its transmembrane domain. After low pH application, insertion of the fusion peptide of HA into the viral membrane provides an additional anchor for the ectodomains of HA. In parallel, recruitment of additional residues to the coiled coil conformation in HA trimers leads to growth of a rigid rod consisting of three α-helices, wrapped around each other. This process exerts forces (f) pulling the anchors toward the growing rod, as illustrated in Fig. 1 *a*, and deforming the membrane.

To analyze the resulting deformation of the membrane, we first consider the shape of a hypothetical particle: the protein within a small fragment of lipid bilayer separated from the rest of the membrane (Fig. 1). The forces f bend the membrane fragment along the lines connecting the anchors and the rod. Most probably, the anchors have limited freedom to move in the membrane plane near the protein, influencing the shape of the membrane fragment and contributing to minimization of the overall energy of the system. We assume that the positions of the three anchors on the imaginary circumference around the protein are to some extent asymmetrical (Fig. 1 *a*). This is a most general assumption, which can be supported by the observation that after low pH activation, the HA trimers become tilted from the membrane normal in the presence or absence of bound target membranes (Tatulian et al., 1995). Such tilting may result from asymmetrical distribution of pulling force with respect to the rigid rod.

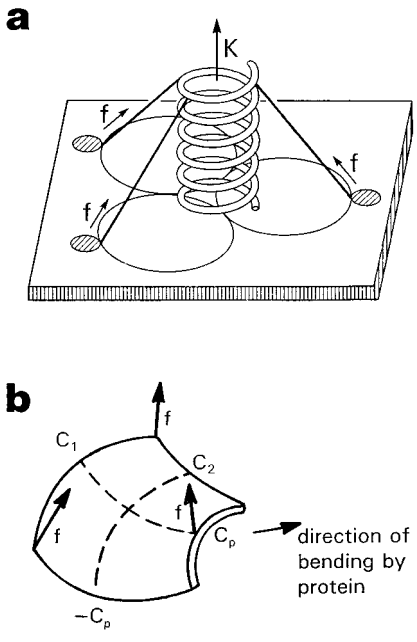

FIGURE 1 Deformation of membrane fragment by activated HA trimer. (*a*) Forces exerted by growing rigid rod on fusion peptides anchored in the host membrane. K is the total force; f is the force acting on each fusion peptide. (*b*) Saddle-like shape adopted by a hypothetically isolated membrane fragment. c_p is the curvature produced by HA; c_1 and c_2 are the principal curvatures.

As a result, the bending produced by the forces f occurs in a particular direction, as illustrated in Fig. 1 *b*, i.e., it has an anisotropic character. We will describe it by the curvature c_p of the membrane surface determined in the direction of the bending (Fig. 1 *b*). The curvature corresponding to bending the membrane toward the α-helical rod (c_p in Fig. 1 *b*) will be defined as positive.

To account for the thermodynamic work A_p performed by the protein in the course of bending, we characterize the action of the forces f by an effective anisotropic bending moment τ_p applied to the unit length of circumference of the membrane fragment. The thermodynamic work by the protein computed per unit area of the membrane fragment is

$$A_p = \tau_p \cdot c_p \tag{1}$$

While the protein performs the work (Eq. 1), an element of the membrane resists deformation because of its bending rigidity κ. The elastic energy accumulated in the course of bending by a unit area of membrane is (Helfrich, 1973)

$$f_b = \frac{1}{2}\kappa \cdot J^2, \tag{2}$$

where J is the total curvature of the fragment of the membrane equal to the sum of the two principal curvatures, $J = c_1 + c_2$.

The total change in the energy per unit area of the membrane fragment consists of the contributions in Eqs. 1 and 2,

$$f = \frac{1}{2}\kappa_p \cdot J^2 - \tau_p \cdot c_p, \tag{3}$$

where the second term is negative, as the thermodynamic work (Eq. 1) performed by the protein corresponds to a decrease in its free energy.

According to Eq. 3, the energy of the membrane fragment is minimal, if the total curvature J remains equal zero, whereas the curvature c_p along the direction of the bending by the protein becomes positive. This conformation can be achieved if the membrane fragment adopts such a shape where one of the principal curvatures, c_1, coincides with

$c_p(c_1 = c_p)$, while the second principal curvature has the opposite value, $c_2 = -c_p$, so that the total curvature vanishes, $J = c_1 + c_2 = 0$. The resulting shape of the membrane fragment is a saddle-like shape illustrated in Fig. 1 *b*. The generation of saddle-like shapes by anisotropic bending properties of membranes has recently been considered by Fournier (1996).

According to our model, the complex of an activated HA trimer with a small portion of lipid bilayer tends to adopt a saddle-like shape, provided that the fusion peptides are inserted into the viral membrane. The energetics of this process is described by Eq. 3.

For the estimate below we need to relate the bending moment τ_p to the total force K exerted by the growing α-helical rigid rod and applied to the anchors and, then, to the energy released as a result of the coiled coil transformation $F_{c\text{-}c}$. An exact relationship between τ_p and K depends on the orientation of the rod with respect to the membrane, a related partition of the total force K between the anchors, a length reached by the rod, and other unknown details. For the qualitative predictions of the present model we will use a simplest relationship following from the dimensional analysis and neglecting all of the details mentioned above, $\tau_p = K$.

An approximate relationship between the total force K and the energy $F_{c\text{-}c}$ can be written as $K = F_{c\text{-}c}/L_{c\text{-}c}$, where $L_{c\text{-}c}$ is the total length the rod reaches as a result of the coiled coil transformation. In this relationship we assume that the total energy $F_{c\text{-}c}$ is gradually released in the course of the whole structural transformation and neglect the possible deviations from this simple scheme. The resulting expression relating the bending moment to the energy of the reaction is

$$\tau_p = \frac{F_{c\text{-}c}}{L_{c\text{-}c}} \tag{4}$$

Ring-like cluster of activated trimers leads to formation of fusion dimple

Although the hypothetical isolated membrane fragment containing an activated HA trimer is free to have the shape of minimal energy, being embedded into a flat lipid bilayer, it is constrained and cannot adopt a saddle-like shape. Indeed, such a process would be related to a strong deformation of the surrounding membrane and, thus, cost energy of membrane bending (Helfrich, 1989). Because it is difficult to determine exactly the resulting shape of the membrane and the corresponding energy, we applied an approximative consideration suggested by Helfrich (1989). The estimate shows that at reasonable values of parameters, the energy price of membrane bending exceeds by far the gain in energy due to the HA-containing membrane fragment acquiring the saddle-like shape. Therefore, we assume that the membrane element with a single activated trimer remains flat despite its tendency to curve. However, a saddle-like deformation becomes possible as a result of the cooperativity of many saddles (Helfrich, 1989). At high surface concentrations of saddles, one expects the formation of an "egg-carton" superstructure of the whole membrane (Helfrich, 1989; Fournier, 1996).

We consider the case of relatively low membrane concentrations of saddles corresponding to the number of HA trimers per unit area of the viral membranes on the order of $10^4/\mu m^2$ (Taylor et al., 1987) and analyze a possibility of local changes in membrane shape driven by self-assembly of the activated trimers in clusters.

We assume the in-plane form of a protein cluster to be a ring (Fig. 2). The inner radius of the ring r_{in} is determined by packing of the trimers. Specifically, we suggest that the minimal HA ring consists of six trimers, as illustrated in Fig. 2. This suggestion is in accord with the conclusion of Blumenthal et al. (1996) and corresponds to the closest packing of the trimers. In this model, the inner radius of the cluster, r_{in}, is close to the radius of the HA trimer r_p. We will assume that r_{in} remains constant in the course of all deformations of the membrane after the formation of the cluster.

The area of the ring A_{cl} is determined by the number of trimers in the cluster, N_A, each trimer having an in-plane area a_p. According to our model, the minimum cluster has an area $A_{cl} = 6a_p$.

The tendency of the ring-like clusters of proteins to adopt a saddle-like shape leads to bulging of the membrane and to formation of a structure called the fusion dimple. The hat-like shape of this dimple (Helfrich, 1989) is illustrated in Fig. 3.

In the dimple the surface covered by the protein cluster with an adjacent (from outside of the protein ring) lipid bilayer has the shape of a funnel (Fig. 3). Such a surface has a saddle-like form at every point and therefore matches the preferred shape of the membrane elements containing the activated trimers. More specifically, we assume that the form of the funnel is that of an axisymmetrical surface with zero total curvature, $J = 0$, called a *catenoid* (axisymmetrical minimal surface; Nitsche, 1975). Because of the vanishing total curvature, such a funnel does not require any bending energy of the membrane. Thus the energy of the funnel is determined solely by the thermodynamic work

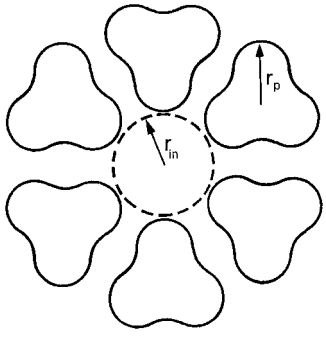

FIGURE 2 Ring-like cluster formed by six HA trimers in the membrane plane.

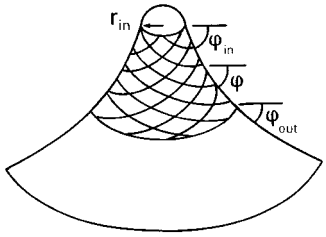

FIGURE 3 Dimple of hat-like shape resulting from bulging of the membrane by the ring-like cluster of activated HA trimers.

performed by the protein molecules,

$$F_f = -\int \tau_p \cdot c_p \cdot dA, \tag{5}$$

where the integral is taken over the area of the protein cluster.

The considered shape of the funnel is an approximation, as in reality, its surface has to deviate from that of a catenoid in the region of transition of the dimple to the undisturbed part of the cell membrane (Petrov and Kozlov, 1984). However, according to the estimate derived in the Appendix, the elastic energy of this transition region is much smaller than the energy of the top of the dimple and, hence, can be neglected.

Moreover, two or more dimples approaching each other can mutually influence the shape of the funnels. In the present qualitative model we will also neglect these corrections.

The top of the fusion dimple closing the funnel has the shape of a part of a sphere, i.e., it is characterized by considerable total curvature J. The saddle-like membrane elements containing the trimers do not enter this region of the membrane because its shape is unfavorable for them. Therefore, the dimple top consists only of a portion of lipid bilayer situated inside the protein cluster (Fig. 3). In contrast to the funnel, the lipidic top is under bending stress related to its curvature J_t, and its elastic energy is

$$F_t = \frac{1}{2}\kappa J_t^2 \cdot A_t, \tag{6}$$

where A_t is the area of the top.

The physical factor driving the bending of the top and, consequently, giving rise to its elastic energy (Eq. 6) is the bending moment τ_p exerted by the activated trimers in the funnel around the top.

We suggest that the bending stress accumulated in the lipidic top facilitates fusion of the dimple with the target membrane. Indeed, hemifusion with the target membrane relieves the bending stress of the outer monolayer of the lipidic top, whereas complete fusion removes the whole bending energy of the lipidic top.

In the following section we analyze the total energy of a dimple F and the bending energy accumulated in its top F_t in terms of the area of a protein cluster A_{cl} and the bending moment τ_p exerted by the proteins. We find the conditions of formation of the dimples and determine the dependence of the number of dimples on the surface concentration c_t of the activated HA trimers.

CRITERIA FOR FORMATION OF FUSION DIMPLES

Elastic energy of fusion dimple

The elastic energy of a fusion dimple is the sum of the energy of the funnel (Eq. 5) and that of the top (Eq. 6), $F = F_f + F_t$.

The meridional curvature c_p of the surface of the catenoid describing the shape of the funnel in Eq. 5 can be expressed through the tangent angle to the profile of the surface φ (Fig. 3),

$$c_p = \frac{1}{r_0}\sin^2\varphi. \tag{7}$$

The area element of the surface of the funnel is given by

$$dA = -2\pi r_0^2 \frac{d\varphi}{\sin^3\varphi}. \tag{8}$$

The parameters r_0 in Eqs. 7 and 8 has the dimension of length and sets the scale of the shape of the catenoid. It can be related to the radius r_{in} and the tangent angle φ_{in} at the inner boundary of the funnel (Fig. 3):

$$r_0 = r_{in} \cdot \sin\varphi_{in}. \tag{9}$$

The curvature J_t and the area A_t of the spherical top of the dimple are determined by r_{in} and φ_{in}, with the assumption that the transition from the top to the funnel is smooth,

$$J_t = -2\frac{\sin\varphi_{in}}{r_{in}}, \qquad A_t = \frac{8\pi}{J_t^2}(1-\cos\varphi_{in}).$$

Taking into account Eqs. 5–9, we obtain the expression for the elastic energy F of the dimple,

$$F = 4\pi\kappa(1-\cos\varphi_{in}) - 2\pi(\tau_p r_{in})\sin\varphi_{in}\log\left[\frac{tg(\varphi_{in}/2)}{tg(\varphi_{out}/2)}\right], \tag{10}$$

where φ_{out} is the tangent angle at the outside boundary of the protein cluster (Fig. 3).

The first term in Eq. 10 gives the energy F_t of the top of the dimple (Eq. 6), and the second term accounts for the energy (Eq. 5) of the cluster of HA trimers.

Integration of Eq. 8 gives a relationship between φ_{in}, φ_{out} and the area A_{cl} of the cluster:

$$\frac{A_{cl}}{\pi r_{in}^2} = \sin^2\varphi_{in}\left(\frac{\cos\varphi_{out}}{\sin\varphi_{out}^2} - \frac{\cos\varphi_{in}}{\sin\varphi_{in}^2} + \log\left[\frac{tg(\varphi_{in}/2)}{tg(\varphi_{out}/2)}\right]\right). \tag{11}$$

To obtain the equilibrium values of the energy (Eq. 10), we have to minimize it with respect to φ_{in}, taking Eq. 11 into account. As a result, we obtain an additional equation,

$$\frac{2\kappa}{\tau_p r_{in}} \sin \varphi_{in} = 1 + \cos \varphi_{in} \cdot \log\left[\frac{tg(\varphi_{in}/2)}{tg(\varphi_{out}/2)}\right] - \left(1 + \cos \varphi_{in} \frac{A_{cl}}{\pi r_{in}^2}\right) \cdot \frac{\sin \varphi_{out}^2}{\sin \varphi_{in}^2}. \quad (12)$$

Solving Eqs. 11 and 12 together, we obtain $\varphi_{in}(A_{cl})$ and $\varphi_{out}(A_{cl})$, determining along with the value of r_{in} the shape of the dimple. Inserting these functions into Eq. 10, we obtain the total energy of the dimple as a function of the area of the protein cluster. This procedure has to be performed numerically, as Eqs. 11 and 12 have no analytical solution. However, in a limiting case of small area of cluster, $A_{cl}/\pi r_{in}^2 \ll 1$, the problem can be solved analytically. We obtain for the values of the tangent angles,

$$\varphi_{in} = \frac{\tau_p r_{in}}{4\kappa} \cdot \frac{A_{cl}}{\pi r_{in}^2}$$

$$\varphi_{out} = \frac{\tau_p r_{in}}{4\kappa} \cdot \frac{A_{cl}}{\pi r_{in}^2}\left(1 - \frac{1}{2}\frac{A_{cl}}{\pi r_{in}^2}\right),$$

and for the energy,

$$F = -\frac{\pi}{8}\frac{(\tau_p r_{in})^2}{\kappa} \cdot \left(\frac{A_{cl}}{\pi r_{in}^2}\right)^2. \quad (13)$$

The energy is negative and increases in its absolute value with the area of the cluster A_{cl}, and with the value of the bending moment of protein τ_p. The dependence of the energy F on the area of protein cluster obtained numerically in a wide range of A_{cl} is presented in Fig. 4.

This analysis suggests that the self-assembly of the trimers in a ring-like cluster accompanied by the dimple formation reduces the elastic energy of the system accounting for the work performed by the activated proteins and the bending energy accumulated in the top of the hat. It means that such structures should form spontaneously.

Bending stress at the top of the dimple

Whereas the change of the total elastic energy F is negative, the bending energy F_t accumulated in the top of the dimple is positive and grows with an increase in the area of the HA cluster and with an increase in the bending moment τ_p. For small areas of the cluster, this energy is

$$F_t = \frac{\pi}{8}\frac{(\tau_p r_{in})^2}{\kappa} \cdot \left(\frac{A_{cl}}{\pi r_{in}^2}\right)^2. \quad (14)$$

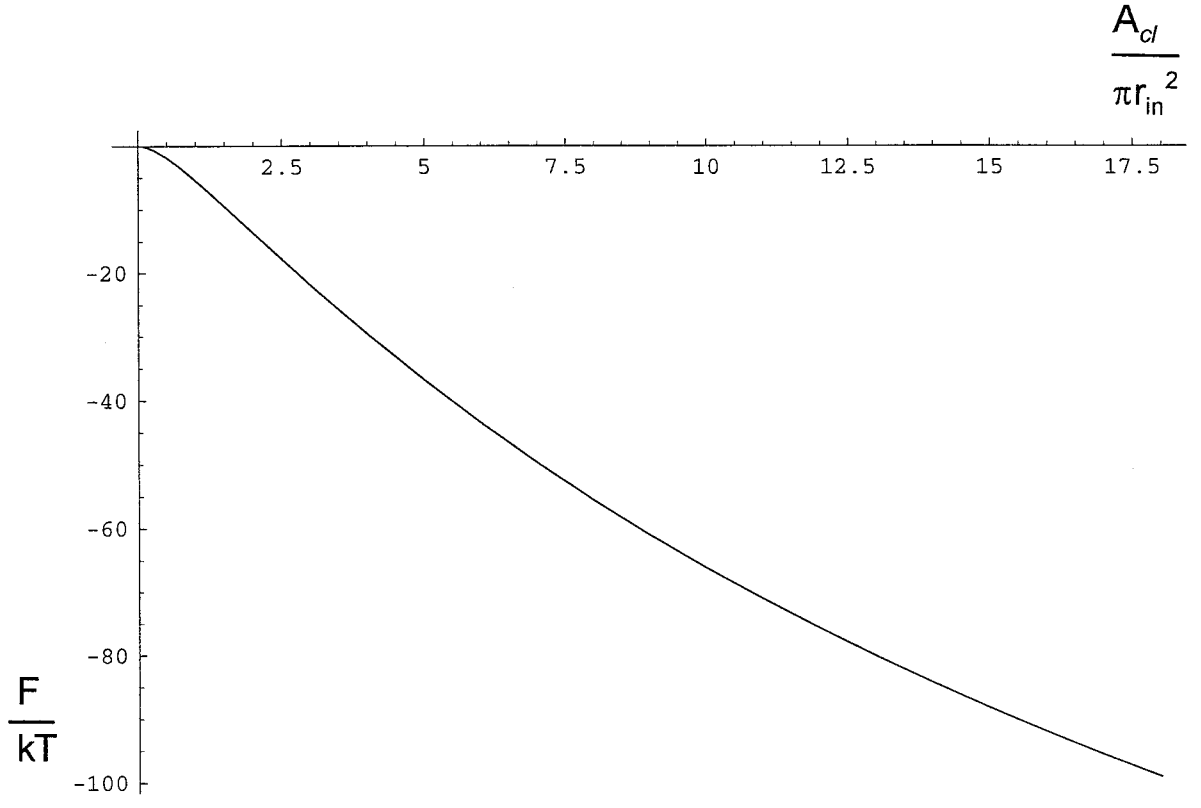

FIGURE 4 Dependence of the energy of fusion dimple F on the area of the ring-like protein cluster A_{cl}, plotted according to Eq. 10. The energy is expressed in the units of kT, where k is the Boltzmann constant and T is the absolute temperature; the area is presented in units of πr_{in}^2, r_{in} being the internal radius of the protein ring. The values of the parameters are $k = 20kT$, $\tau_p r_{in}/2\kappa = 0.6$.

Fig. 5 illustrates the behavior of F_t in a wide range of A_{cl}.

Number of fusion dimples

The number of protein clusters giving rise to the dimples is determined by the surface concentration of the activated trimers c_t.

To find this dependence, we consider the thermodynamic equilibrium between the proteins in clusters and the single protein molecules remaining in the membrane. At equilibrium, a decrease in the elastic energy of the system F resulting from transfer of an additional HA trimer to a cluster is compensated for by the loss of translational entropy of proteins. It can be expressed in common terms as the condition of equal chemical potential of an HA trimer in a cluster, μ_A, and that of a single trimer, μ_m. For the clusters consisting of $N = A_{cl}/a_p$ trimers, this condition can be presented as

$$\mu_m^0 + kT \ln c_m = \mu_A^0(A_{cl}) + kT \frac{a_p}{A_{cl}} \ln c_A^N, \qquad (15)$$

where c_A^N is the surface concentration of the clusters of this kind, and kT is the product of the Boltzmann constant and the absolute temperature. The terms proportional to kT on the left and right sides of (15) determine the contributions of the translational entropy to the chemical potentials of the single and aggregated HA trimers, respectively. The terms $\mu_p^0(A_{cl})$ and μ_m^0 describe the contribution to μ_A and μ_m from all intramembrane interactions.

In addition to Eq. 15, we use the condition of a given total concentration c_t of the activated HA trimers, expressed by

$$c_m + \sum_{A_{cl}^{min}}^{\infty} c_A^N \cdot \frac{A_{cl}}{a_p} = c_t, \qquad (16)$$

where the sum is taken over all possible areas of cluster, starting from its minimum value A_{cl}^{min}.

Equations 15 and 16 allow us to relate the concentration of clusters c_A^N to the total concentration of proteins c_t, provided that the difference between $\mu_p^0(A_{cl})$ and μ_m^0 is known.

We assume that the difference $\Delta\mu(A_{cl}) = \mu_A^0(A_{cl}) - \mu_m^0$ is determined only by the change in the elastic energy F resulting from the transfer of one trimer to a cluster. Then we can write

$$\Delta\mu(A_{cl}) = a_p \frac{\partial F}{\partial A_{cl}}.$$

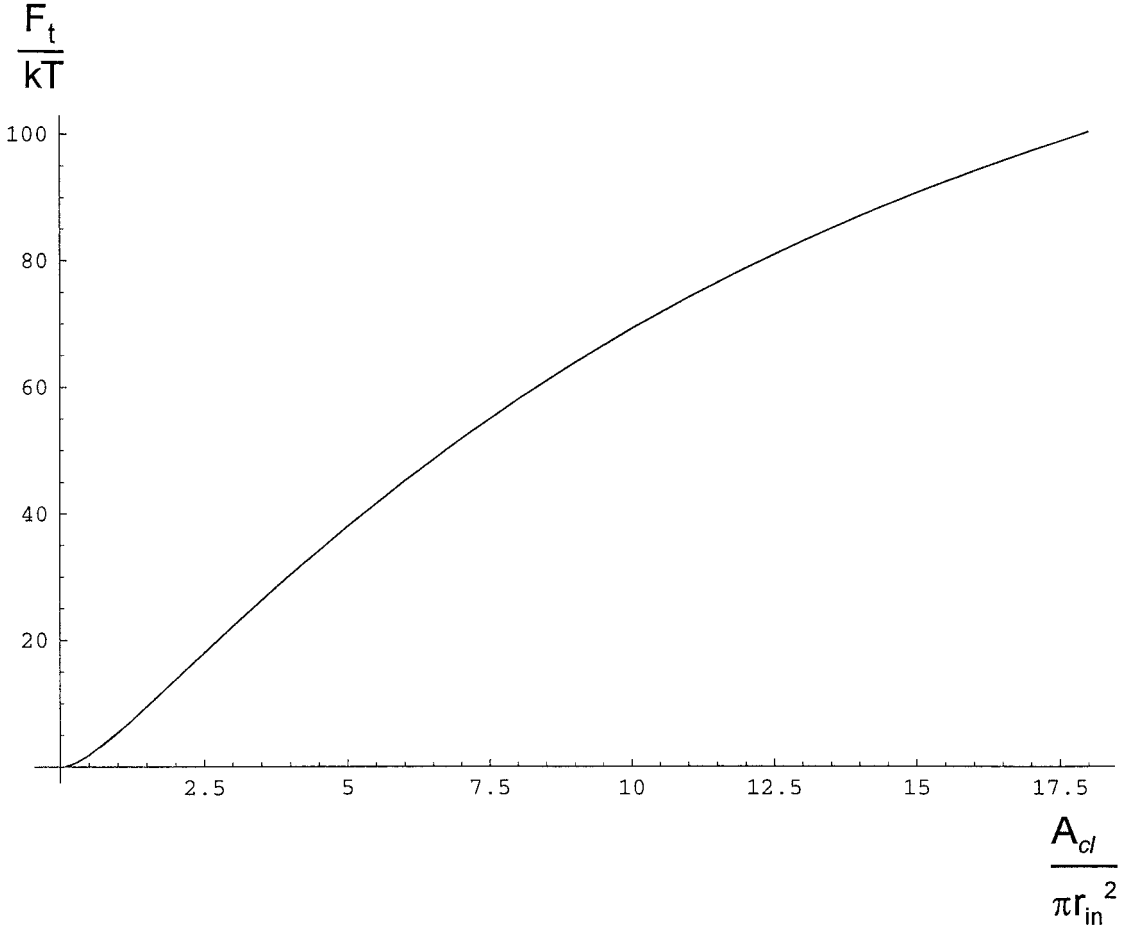

FIGURE 5 Dependence of the energy of the lipidic top of the fusion dimple F_t on the area of the ring-like cluster F_t. The units and the values of parameters are as in Fig. 4.

Differentiation of Eq. 10, taking into account Eqs. 11 and 12, gives

$$\Delta\mu(A_{cl}) = -a_p \frac{\tau_p}{r_{in}} \frac{\sin^2\varphi_{out}}{\sin\varphi_{in}}, \quad (17)$$

where the values φ_{out} and φ_{in} are the solutions of Eqs. 11 and 12. Because the angle φ_{in} cannot exceed π, the difference $\Delta\mu(A_{cl})$ is negative. This confirms again the tendency of the proteins to aggregate.

The behavior $\Delta\mu(A_{cl})$ illustrated in Fig. 6 has a nonmonotonic character. However, the minimum of this curve for all reasonable values of parameters corresponds to the normalized area of the cluster $A_{cl}/\pi r_{in}^2 \approx 2$, which is smaller than the normalized area of the minimal cluster $A_{cl}/\pi r_{in}^2 = 6$ considered in our model. Therefore, for practical purposes the function $\Delta\mu(A_{cl})$ can be seen as negative and decreasing monotonically in its absolute value, approaching zero for $A_{cl}/\pi r_{in}^2 \to \infty$.

Equations 15 and 16, determining the surface concentration of clusters, are analogous to the problem of formation of micelles of surfactant in aqueous solution (Tanford, 1980). In analogy to the well-known results of this theory, we conclude from Eqs. 15 and 16 that the concentration of the clusters c_A^N decreases exponentially with the number of aggregated trimers N. Therefore, we will neglect all of the clusters larger than the minimal ones with the aggregation number $N_{min} = 6$. The concentration c_A^* of these clusters is then determined by the equation

$$c_t = 6 \cdot c_A^* + (c_A^*)^{1/6} \cdot \exp[\Delta\mu(A_{cl}^{min})]. \quad (18)$$

Numerical solution of Eq. 18 is illustrated in Fig. 7. The surface concentration of clusters c_A^* increases with the total concentration of the activated trimers c_t. For the total concentration exceeding a particular value c_t^* (analogous to the critical micelle concentration (*cmc*) in the case of surfactant micelles), c_A^* reaches the same order of magnitude as c_t. For the values of parameters used in Fig. 7 and discussed below, the value of c_t^* is ~1000 trimers/μm^2.

DISCUSSION

Low pH-activated HA efficiently fuses two lipid bilayers into one. Although a great deal is known about the low pH-induced major refolding of HA, and the rearrangements

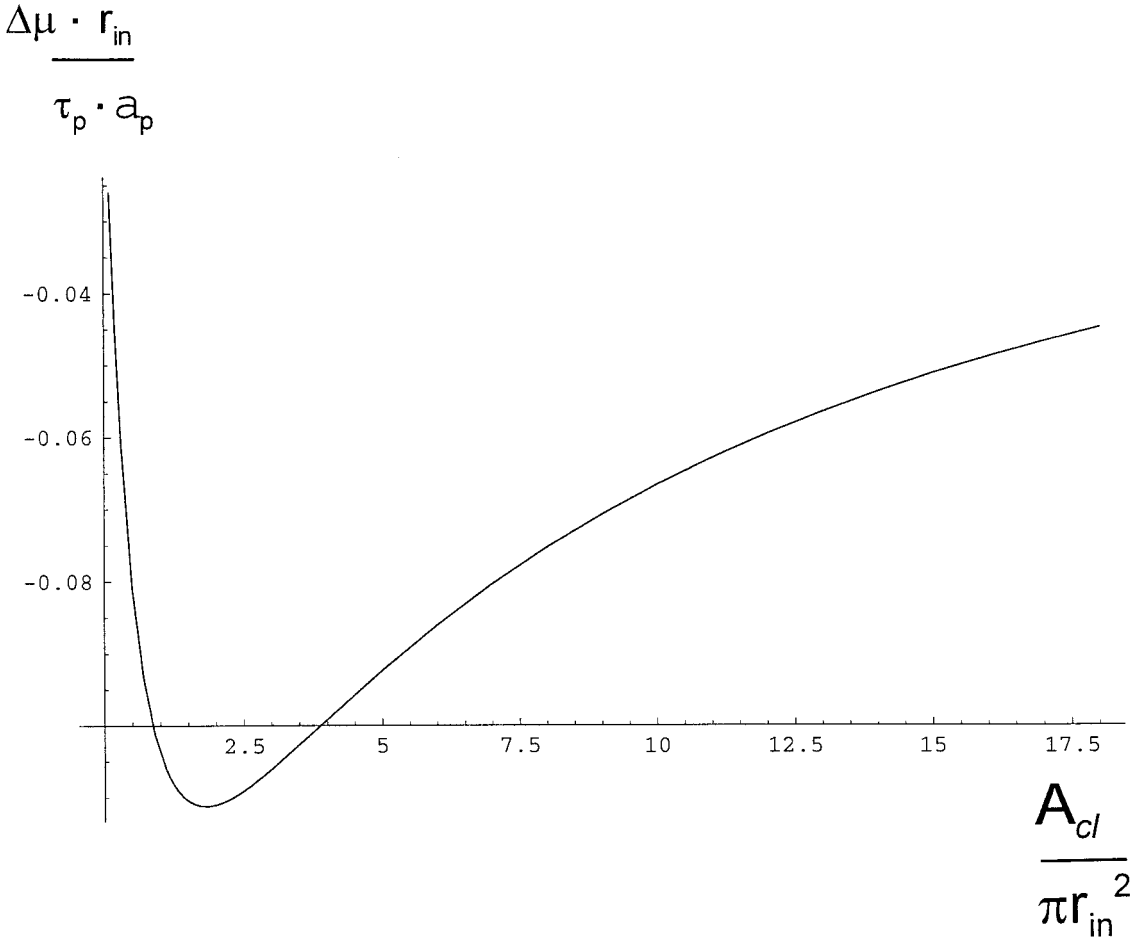

FIGURE 6 Dependence of the chemical potential of HA trimer in cluster μ_p on the area of the cluster A_{cl}. μ_p is expressed in units of $\tau_p a_p / r_{in}$. The values of parameters are as in Fig. 4.

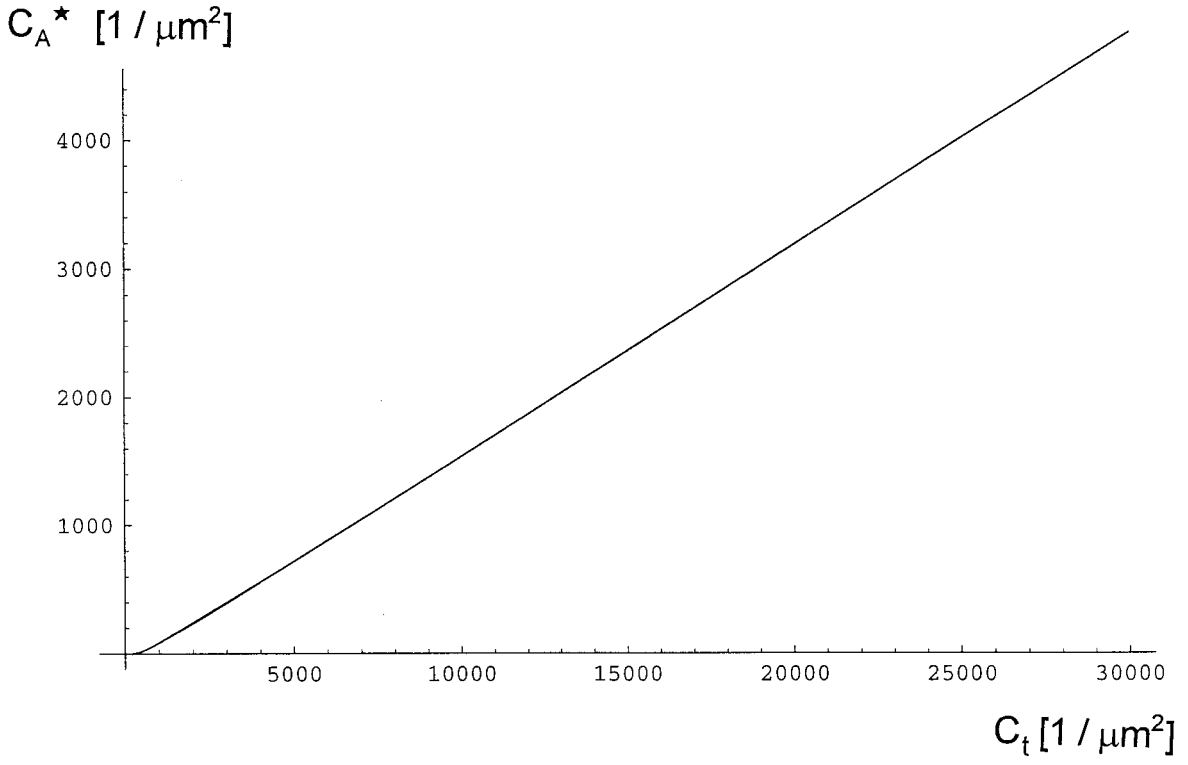

FIGURE 7 Dependence of the surface density of fusion dimples c_A^* on the total surface density of the activated HA trimers c_t. The values of parameters are $N = 6$, $r_{in} = r_p = 4$ nm, $F_{c\text{-}c} = 60kT$, $L_{c\text{-}c} = 10$ nm.

of the lipid bilayers in fusion, a missing link is the coupling between these two processes. In the present work we suggest a scenario by which the activated fusion proteins such as HA can produce viral membrane dimples surrounded by a ring-like cluster of HA and committed to fusion with the target membrane.

We hypothesize that acidification of HA trimers triggers insertion of their fusion peptides into the viral membrane. The subsequent extension of a rigid coiled coil conformation exerts a force that bends the viral membrane. The resulting tendency of membrane elements containing activated HA to adopt a saddle-like shape drives self-assembly of the proteins in a ring-like cluster, and formation of a membrane dimple directed toward the target membrane. The growth of this dimple can provide a very close local contact between the membranes initially separated by a distance of 10 nm, which is too large for fusion. The bending stresses at the top of the growing dimple facilitate its fusion with the target membrane. Because HA molecules are excluded from the top of the dimple, fusion of the lipidic bilayers of the viral membrane and the target membrane depends on membrane lipids, as does fusion of protein-free lipid bilayers.

Fusion peptides of low-pH activated HA molecules insert into both target and viral membranes (Gaudin et al., 1995; Weber et al., 1994). We suggest the mechanism by which the insertion of the fusion peptides into the viral membrane can cause membrane fusion. In previous studies this process has been associated with an inactivation of HA, leading to the loss of its ability to induce fusion (see, for a review, Gaudin et al., 1995). In contrast, insertion of the peptide into the target membrane has been hypothesized to lead to productive, fusion-competent HA conformations. In our model insertion of the fusion peptides into a viral membrane along with the extension of the coiled coil conformation are responsible for the protein clusterization, membrane bulging, and accumulation of the bending stresses leading to fusion.

Basic estimates

Let us estimate whether the model gives reasonable predictions for real values of parameters. The bending energy of the top of a dimple, F_t, and the number of the dimples formed per unit area of the membrane, c_A^*, depend mainly on the energy of the coiled coil transformation, $F_{c\text{-}c}$, and the surface density of the activated proteins, c_t. Additional parameters important for the qualitative estimates are the length of the rod reached as a result of the coiled coil transformation $L_{c\text{-}c}$, the radius of the lipid spot inside the protein ring r_{in}, the in-plane radius of an HA monomer r_p, and the bending rigidity of the membrane κ.

The maximum length of the rod is assumed to be $L_{c\text{-}c} \simeq 10$ nm (Bullough et al., 1994); the radius r_{in}, approximately equal in our model to the in-plane radius of one HA trimer, is $r_{in} = r_p \simeq 4$ nm (Wiley and Skehel, 1987); the bending

modulus of the bilayer is assumed to be $\kappa = 20kT$ (Niggemann et al., 1995). To estimate the energy $F_{c\text{-}c}$, we use the hypothesis (Carr and Kim, 1993; Bullough et al., 1994) that the transition of an HA trimer from initial to low pH conformation involves the extension of the preexisting three-stranded coiled coil to include the loop regions and the short, external α-helices. This reaction involves transition of ~6 heptads of each of the three HA_2 subunits to the coiled coil conformation (Carr and Kim, 1993; Bullough et al., 1994). The free energy of the coiled coil transition can be estimated as 1–2 kcal/mol for one heptad (Boice et al., 1996; Jelesarov and Bosshard, 1996; Krylov et al., 1994). Assuming the transition energy of 2 kcal/mol, the estimate of $F_{c\text{-}c}$ for one HA trimer gives $F_{c\text{-}c} = 60kT$. The estimate of the corresponding total force and bending moment exerted by the growing rod gives $K = \tau_p = F_{c\text{-}c}/L_{c\text{-}c} \simeq 2.4 \cdot 10^{-11}$ N. The force pulling each of the three fusion peptides inserted into the membrane is on the order of $f \simeq 8 \times 10^{-12}$ N.

The question can arise, whether the tightness of binding of the anchors (fusion peptides) to the membrane is sufficiently strong that the pulling of the anchors by the growing rod does not detach them from the membrane. To estimate the energy of such an attachment, we use the binding constant of a fusogenic synthetic peptide to phospholipid bilayers, determined by Ishiguro et al., (1996). For neutral pH this value is 42.5 mM^{-1} (Ishiguro et al., 1996), which gives the energy of attachment of ~15kT per fusion peptide. The length of a fusion peptide is ~3 nm (Ishiguro et al., 1996). The resulting force needed to detach the fusion peptide is 2×10^{-11} N, which is larger than the pulling force estimated above. It is noteworthy that in acidic conditions the force of attachment of the fusion peptide to the membrane can be even larger, because of an increase in hydrophobicity of the molecule and a change in its orientation in the membrane (Ishiguro et al., 1996).

According to our model, the bending energy $F_t = 4\pi\kappa(1 - \cos \varphi_{in})$ accumulated at the top of the dimple and released during its fusion with the target membrane increases with the energy of the coiled coil transition $F_{c\text{-}c}$ and the number of trimers composing the ring-like cluster. For the value $F_{c\text{-}c} \simeq 60kT$, and in the case of six trimers in the cluster, the inner tangent angle resulting from solution of Eqs. 11 and 12 is $\varphi_{in} \simeq 0.6$, and the estimated bending energy F_t is ~45kT. Even this lowest estimate of F_t is close to the energy required to locally merge the contacting monolayers of two membranes in a fusion intermediate called the stalk (Kozlov and Markin, 1983; Siegel, 1993). The energy of this intermediate was estimated as in Siegel (1993), using 10kT for the bending modulus of monolayer (Niggemann et al., 1995). Thus the bending stresses at the top of the dimple are sufficiently strong to facilitate fusion.

Fig. 7 presents the dependence of the surface density of the fusion dimples c_A^* as a function of the density of the activated HA trimers c_t, assuming the energy of the coiled coil extension $F_{c\text{-}c} = 60kT$. If c_t changes in a range from 1000 to 30,000 trimers/μm^2, which corresponds to HA densities in HA-expressing cells (Danieli et al., 1996) and in viral envelopes (Taylor et al., 1987), respectively, the density of the dimples changes drastically from just a few to ~5000/μm^2. The characteristic area of contact of virus with the target membrane is on the order of 0.002 μm^2, assuming the radius of the contact area to be ~25 nm. If all HA molecules in this area are activated, the number of dimples in the contact area will be ~10. If only 50% of HA are activated, we still can expect about five dimples in the contact zone. A similar number of dimples (two dimples) can be expected in cell-cell fusion mediated by HA, assuming a contact area of 1 μm^2, and a surface density of HA of 1000 trimers/μm^2 with half of them activated. This estimate shows that the surface density of HA in viral particles and in HA-expressing cells is sufficient to promote dimple formation.

Although this analysis suggests that the hypothetical mechanism developed here is consistent with many experimental findings on HA-mediated fusion, our model is clearly oversimplified. For instance, the only role for the fusion peptide in this model is to hold the HA ectodomain to the viral membrane while the HA trimer undergoes refolding. On the other hand, it is known that the interaction of the isolated fusion peptide with lipids alters the elastic properties of lipid monolayers and destabilizes bilayer structure (Rafalski et al., 1991; Epand and Epand, 1994; Luneberg et al., 1995). We also ignore the possibility of additional molecular interactions between HAs in the cluster. Note, however, that the HA interactions in the cluster should not be too strong to allow its breaking by expansion of the fusion pore. The close contact between viral and target membranes can also affect both the conformational changes in HA in the fusion site and the dimple development. The inactivation of HA with time after low pH application (Duzgunes et al., 1992; Ramalho-Santos et al., 1993; Korte et al., 1997) is also neglected here, as are all kinetic aspects of the protein assembly, dimple development, and lipid bilayer fusion.

Conclusions and possible verifications of the model

Despite the striking diversity of different biological fusion processes, the actual rearrangements of membrane lipid bilayers apparently proceed via similar lipid-involving intermediates (Chernomordik et al., 1995b; Monck and Fernandez, 1992), and the proteins that mediate fusion can share important structural motifs (Hernandez et al., 1996). The hypothetical mechanism of the protein-mediated fusion discussed here for HA-mediated fusion can work in other fusion processes. A similar scenario has been suggested for exocytosis by Monck and Fernandez (1992). In their "scaffold" model, unidentified fusion proteins surrounding a fusion site induce dimpling of the plasma membrane toward the granule membrane, and provide the bending stress of the tip of the dimple to promote its fusion. Our model suggests

a specific physical mechanism of these processes for a well-characterized protein.

We focused here on the illustration of the main idea and the most important predictions of the model, such as the crucial role of insertion of the fusion peptide into the viral membrane and HA-dependent dimpling of viral membrane in the fusion site. Dimple formation by the described mechanism can explain electron microscopic observations of deformed influenza virus particles with angular or undulating membranes (Ruigrok et al., 1992) and with discontinuities and bleb-like structures (Shangguan et al., 1997) observed at low pH. Importantly, these structures appear at significant numbers only after 10 min of incubation at low pH (Shangguan et al., 1997), indicating that viral envelope dimples, if they exist and are required for fusion, are rather infrequent, small, and transient structures. If formation of a membrane dimple did not result in fusion (for instance, in the absence of the target membrane), refolding of HA into the final low pH conformation would eventually yield inactivated molecules with discharged spring "engines." We hope that the future morphological and structural characterization of the fusion intermediates arrested downstream from the low pH application (Schoch et al., 1992; Chernomordik et al., 1997) will allow us to verify whether fusion is preceded by the formation of a membrane dimple. The specific dependence of the dimple number and, correspondingly, fusion rate on the surface density of the activated trimers (Fig. 7) can be tested experimentally by altering either the pH applied, or the surface density of HA competent for low-pH activation (Clague et al., 1991; Danieli et al., 1996).

Two other important parameters of the system can be changed experimentally by mutagenesis. The first is the length of the hairpin loop sequence having a high propensity for forming a coiled coil. Variation of this parameter will change the energy released in the low-pH-induced extension of the coiled coil and, thus, the bending moment τ_p exerted by the protein. The second is the structure of the fusion peptide determining the strength of its attachment to the membrane. Reduction of the energy of this attachment should eliminate formation of the fusion dimples.

We hope that further experimentation and development of the physical models of biological fusion will help researchers better understand the correlation of the structure of fusion proteins with their function as catalysts of lipid bilayer rearrangements.

APPENDIX

In this section we estimate the elastic energy of the transition region between the dimple and the flat membrane. We model the shape of this region as a segment of a regular circular toroid connected to the catenoidal funnel at the radial coordinate $\tilde{R}$, as illustrated in Fig. 8. Transition from the funnel to the toroid is smooth, so that the tangent angle φ remains constant at $\tilde{R}$.

In contrast to the funnel, the total curvature of the toroid is different from zero, and its formation requires elastic energy F_{ext}. To compute this energy, we recall that the shape of the funnel of zero total curvature is given by (Helfrich, 1989)

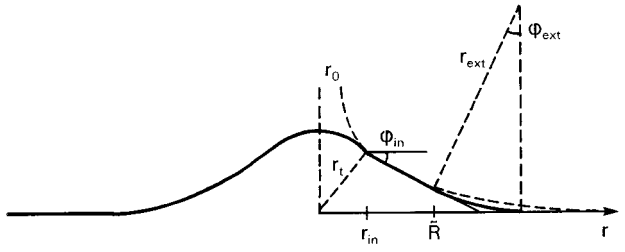

FIGURE 8 Cross section of a dimple, including the toroidal region of transition from funnel to flat membrane.

$$z = z_0 - r_0 \cdot \log\left[\frac{r}{r_0} + \sqrt{\frac{r^2}{r_0} - 1}\right], \tag{A1}$$

where r is the radial coordinate and r_0 is determined by Eq. 9.

The total height H of the dimple involving the contributions of the spherical top, the funnel, and the toroidal segment is

$$H = r_t(1 - \cos\varphi_{in}) + r_0 \cdot \log\left[\frac{\tilde{R}}{r_0} + \sqrt{\frac{\tilde{R}^2}{r_0} - 1}\right] - r_0 \cdot \log\left[\frac{r_{in}}{r_0} + \sqrt{\frac{r_{in}^2}{r_0} - 1}\right] + r_{ext}(1 - \cos\varphi_{ext}), \tag{A2}$$

where r_{in} and φ_{in} are introduced in the main section, $r_t = r_{in}/\sin\phi_{in}$ is the curvature radius of the spherical top, r_{ext} is the radius of the toroidal segment cross section, and φ_{ext} is its arc angle.

Denoting the arc length of the toroidal cross section by l, using Eq. A1, and assuming the tangent angle φ to be small, we express approximately the geometrical characteristics of the toroidal segment by

$$\varphi_{ext} = \frac{r_0}{\tilde{R}} \tag{A3}$$

$$r_{ext} = \frac{l}{\varphi_{ext}} = \frac{l \cdot \tilde{R}}{r_0}, \tag{A4}$$

and its area by

$$A_{ext} = 2\pi\tilde{R} \cdot l. \tag{A5}$$

We estimate the energy of the toroidal segment as

$$F_{ext} = \frac{1}{2}\kappa \cdot A_{ext} \cdot \frac{1}{r_{ext}^2}. \tag{A6}$$

This expression overestimates the energy, as it neglects the contribution of the second principal curvature of the toroidal surface, which is smaller than $1/r_{ext}$ in its absolute value, but has an opposite sign and, hence, results in a decrease in the elastic energy.

Inserting Eqs. A4 and A5 into Eq. A6, we obtain

$$F_{ext} = \pi\kappa \frac{r_0^2}{l\tilde{R}}. \tag{A7}$$

The energy (Eq. A7) has to be minimized with respect to the coordinate $\tilde{R}$ of transition from the funnel to the toroidal segment, taking into account the relationship between l and $\tilde{R}$ given implicitly by Eq. A2. Inserting Eqs.

A3, and A4 into Eq. A2, we obtain a differential form of this relationship,

$$\frac{d\tilde{R}}{dl} = -\frac{1}{2}\frac{1}{1 - 1/2\tilde{R}}.$$

The energy minimization accounting for $r_0/\tilde{R} \ll 1$ results in $l = \tilde{R}$, so that the energy of the toroidal segment is

$$F_{ext} = \pi\kappa \cdot \frac{r_0^2}{\tilde{R}^2}. \quad \text{(A8)}$$

Using the obtained relationships together with Eqs. A2–A4 and Eq. 9, we find

$$\tilde{R} = \frac{1}{2} r_{in} \cdot (1 + \cos \varphi_{in}) \cdot \exp\left[-\left(\frac{1}{2} + \frac{1 - \cos \varphi_{in}}{\sin^2 \varphi_{in}}\right)\right] \cdot \exp\left[\frac{H}{r_{in} \sin \varphi_{in}}\right]. \quad \text{(A9)}$$

The value of the angle of the spherical cap resulting from the calculations of the main part is $\varphi_{in} \simeq 0.6$. We assume the height of the dimple to be $H = 10$ nm, whereas the value of r_{in} is taken to be equal to 4 nm.

Using these values in Eq. A9, we obtain $\tilde{R} \simeq 100$ nm. Taking into account $l = \tilde{R}$, the radius of dimple projection on the plane of flat membrane can be estimated as $2\tilde{R} \simeq 200$ nm.

Inserting the obtained value for $\tilde{R}$ together with Eq. 9 into Eq. A8, we estimate the energy of the transition region from the funnel to the flat membrane as

$$F_{ext} \simeq 5 \times 10^{-4} \pi\kappa. \quad \text{(A10)}$$

This energy is much smaller than the energy of the spherical top,

$$F_t = 4 \cdot (1 - \cos \varphi_{in}) \pi\kappa \simeq 0.7 \pi\kappa, \quad \text{(A11)}$$

and hence is neglected in the main part of this paper.

Let us emphasize that we estimated the upper limit of the energy of the transition region. In the case of a virus particle whose dimension is lower than the estimated base of the dimple, transition from the funnel to the surrounding membrane does not require formation of a toroidal segment and, hence, is not related even to the small energy (Eq. A10).

We thank Drs. Gregory Melikyan and Joshua Zimmerberg for critical reading of the manuscript and helpful discussions.

REFERENCES

Alford, D., H. Ellens, and J. Bentz. 1994. Fusion of influenza virus with sialic acid-bearing target membranes. *Biochemistry.* 33:1977–1987.

Bentz, J., H. Ellens, and D. Alford. 1990. An architecture for the fusion site of influenza hemagglutinin. *FEBS Lett.* 276:1–5.

Blumenthal, R., C. C. Pak, Y. Raviv, M. Krumbiegel, L. D. Bergelson, S. J. Morris, and R. J. Lowy. 1995. Transient domains induced by influenza hemagglutinin during membrane fusion. *Mol. Membr. Biol.* 12:135–142.

Blumenthal, R., D. P. Sarkar, S. Durell, D. E. Howard, and S. J. Morris. 1996. Dilation of the influenza hemagglutinin fusion pore revealed by the kinetics of individual cell-cell fusion events. *J. Cell Biol.* 135:63–71.

Boice, J. A., G. R. Dieckmann, W. F. DeGrado, and R. Fairman. 1996. Thermodynamic analysis of a designed three-stranded coiled coil. *Biochemistry.* 35:14480–14485.

Bullough, P. A., F. M. Hughson, J. J. Skehel, and D. C. Wiley. 1994. Structure of influenza hemagglutinin at the pH of membrane fusion. *Nature.* 371:37–43.

Carr, C. M., and P. S. Kim. 1993. A spring-loaded mechanism for the conformational change of influenza hemagglutinin. *Cell.* 73:823–832.

Chanturiya, A., L. V. Chernomordik, and J. Zimmerberg. 1997. Flickering fusion pores comparable to initial exocytotic pores occur in protein-free phospholipid bilayers. *Proc. Natl. Acad. Sci. USA.* (in press).

Chernomordik, L. V., V. A. Frolov, E. Leikina, P. Bronk, and J. Zimmerberg. 1998. The pathway of membrane fusion catalyzed by influenza hemagglutinin: restriction of lipids, hemifusion, and lipidic fusion pore formation. *J. Cell Biol.* (in press).

Chernomordik, L., A. Chanturiya, J. Green, and J. Zimmerberg. 1995a. The hemifusion intermediate and its conversion to complete fusion: regulation by membrane composition. *Biophys. J.* 69:922–929.

Chernomordik, L., M. M. Kozlov, and J. Zimmerberg. 1995b. Lipids in biological membrane fusion. *J. Membr. Biol.* 146:1–14.

Chernomordik, L. V., E. Leikina, V. Frolov, P. Bronk, and J. Zimmerberg. 1997. An early stage of membrane fusion mediated by the low pH conformation of influenza hemagglutinin depends upon membrane lipids. *J. Cell Biol.* 136:81–94.

Clague, M. J., C. Schoch, and R. Blumenthal. 1991. Delay time for influenza virus hemagglutinin-induced membrane fusion depends on hemagglutinin surface density. *J. Virol.* 65:2402–2407.

Danieli, T., S. L. Pelletier, Y. I. Henis, and J. M. White. 1996. Membrane fusion mediated by the influenza virus hemagglutinin requires the concerted action of at least three hemagglutinin trimers. *J. Cell Biol.* 133:559–569.

Duzgunes, N., M. C. Pedroso de Lima, L. Stamatatos, D. Flasher, D. Alford, D. S. Friend, and S. Nir. 1992. Fusion activity and inactivation of influenza virus: kinetics of low pH-induced fusion with cultured cells. *J. Gen. Virol.* 73:27–37.

Epand, R. M., and R. F. Epand. 1994. Relationship between the infectivity of influenza virus and the ability of its fusion peptide to perturb bilayers. *Biochem. Biophys. Res. Commun.* 202:1420–1425.

Fournier, J. B. 1996. Nontopological saddle-splay and curvature instabilities from anisotropic membrane inclusions. *Phys. Rev. Lett.* 76: 4436–4439.

Gaudin, Y., R. W. H. Ruigrok, and J. Brunner. 1995. Low-pH induced conformational changes in viral fusion proteins: implications for the fusion mechanism. *J. Gen. Virol.* 76:1541–1556.

Guy, H. R., S. R. Durell, C. Schoch, and R. Blumenthal. 1992. Analyzing the fusion process of influenza hemagglutinin by mutagenesis and molecular modeling. *Biophys. J.* 62:95–97.

Helfrich, W. 1973. Elastic properties of lipid bilayers: theory and possible experiments. *Z. Naturforsch.* 28c:693–703.

Helfrich, W. 1989. Hats and saddles in lipid membranes. *Liquid Crystals.* 5:1647–1658.

Hernandez, L. D., L. R. Hoffman, T. G. Wolfberg, and J. M. White. 1996. Virus-cell and cell-cell fusion. *Annu. Rev. Cell Dev. Biol.* 12:627–661.

Hughson, F. M. 1995. Structural characterization of viral fusion proteins. *Curr. Biol.* 5:265–274.

Ishiguro, R., M. Matsumoto, and S. Takahashi. 1996. Interaction of fusogenic synthetic peptide with phospholipid bilayers: orientation of the peptide α-helix and binding isotherm. *Biochemistry.* 35:4976–4983.

Jelesarov, I., and H. R. Bosshard. 1996. Thermodynamic characterization of the coupled folding and association of heterodimeric coiled coils (leucine zippers). *J. Mol. Biol.* 263:344–358.

Kemble, G. W., T. Danieli, and J. M. White. 1994. Lipid-anchored influenza hemagglutinin promotes hemifusion, not complete fusion. *Cell.* 76:383–391.

Korte, T., K. Ludwig, M. Krumbiegel, D. Zirwer, G. Damaschun, and A. Herrmann. 1997. Transient changes of the conformation of hemagglutinin of influenza virus at low pH detected by time-resolved circular dichroism spectroscopy. *J. Biol. Chem.* 272:9764–9770.

Kozlov, M. M., and V. S. Markin. 1983. Possible mechanism of membrane fusion. *Biofizika.* 28:242–247.

Krylov, D., I. Mikhailenko, and C. Vinson. 1994. A thermodynamic scale for leucine zipper stability and dimerization specificity: e and g interhelical interactions. *EMBO J.* 13:2849–2861.

Lee, J., and B. R. Lentz. 1997. Evolution of lipidic structures during model membrane fusion and the relation of this process to cell membrane fusion. *Biochemistry.* 36:6251–6259.

Luneberg, J., I. Martin, F. Nussler, J. M. Ruysschaert, and A. Herrmann. 1995. Structure and topology of the influenza virus fusion peptide in lipid bilayers. *J. Biol. Chem.* 270:27606–27614.

Melikyan, G. B., and L. V. Chernomordik. 1997. Membrane rearrangements in fusion mediated by viral proteins. *Trends Microbiol.* 5:349–355.

Melikyan, G. B., J. M. White, and F. S. Cohen. 1995. GPI-anchored influenza hemagglutinin induces hemifusion to both red blood cell and planar bilayer membranes. *J. Cell Biol.* 131:679–691.

Monck, J. R., and J. M. Fernandez. 1992. The exocytotic fusion pore. *J. Cell Biol.* 119:1395–1404.

Nanavati, C., V. S. Markin, A. F. Oberhauser, and J. M. Fernandez. 1992. The exocytotic fusion pore modeled as a lipidic pore. *Biophys. J.* 63:1118–1132.

Niggemann, G., M. Kummrow, and W. Helfrich. 1995. The bending rigidity of phosphatidylcholine bilayers: dependences on experimental method, sample cell sealing and temperature. *J. Phys. France.* 5:413–425.

Nitsche, J. C. C. 1975. Vorlesung über Minimalflächen. Springer-Verlag, Berlin, Heidelberg, New York.

Petrov, A. G., and M. M. Kozlov. 1984. Curvature elasticity and passage formation in lipid bilayer lattice of passages. *C. R. Bulg. Acad. Sci.* 37:1191–1193.

Pevsner, J., and R. H. Scheller. 1994. Mechanisms of vesicle docking and fusion: insights from the nervous system. *Curr. Opin. Cell. Biol.* 6:555–560.

Rafalski, M., A. Ortiz, A. Rockwell, L. C. van Ginkel, J. D. Lear, W. F. DeGrado, and J. Wilschut. 1991. Membrane fusion activity of the influenza virus hemagglutinin: interaction of HA2 N-terminal peptides with phospholipid vesicles. *Biochemistry.* 30:10211–10220.

Ramalho-Santos, J., S. Nir, N. Duzgunes, A. P. de Carvalho, and M. d. C. de Lima. 1993. A common mechanism for influenza virus fusion activity and inactivation. *Biochemistry.* 32:2771–2779.

Ruigrok, R. W., E. A. Hewat, and R. H. Wade. 1992. Low pH deforms the influenza virus envelope. *J. Gen. Virol.* 73:995–998.

Schoch, C., R. Blumenthal, and M. J. Clague. 1992. A long-lived state for influenza virus-erythrocyte complexes committed to fusion at neutral pH. *FEBS Lett.* 311:221–225.

Shangguan, T., D. P. Siegel, J. D. Lear, P. H. Axelsen, and J. Bentz. 1997. Morphological changes and fusogenic activity of the influenza virus hemagglutinin. *Biophys. J.* 74:54–62.

Siegel, D. P. 1993. Energetics of intermediates in membrane fusion: comparison of stalk and inverted micellar mechanisms. *Biophys. J.* 65: 2124–2140.

Siegel, D. P., and R. M. Epand. 1997. The mechanism of lamellar-to-inverted hexagonal phase transitions in phosphatidylethanolamine: implications for membrane fusion mechanisms. *Biophys. J.* 73:3089–3111.

Stegmann, T. 1993. Influenza hemagglutinin-mediated membrane fusion does not involve inverted phase lipid intermediates. *J. Biol. Chem.* 268:1716–1722.

Stegmann, T., J. M. White, and A. Helenius. 1990. Intermediates in influenza induced membrane fusion. *EMBO J.* 9:4231–4241.

Tanford, C. 1980. The Hydrophobic Effect—Formation of Micelles and Biological Membranes, 2nd Ed. John Wiley and Sons, New York.

Tatulian, S. A., P. Hinterdorfer, G. Baber, and L. K. Tamm. 1995. Influenza hemagglutinin assumes a tilted conformation during membrane fusion as determined by attenuated total reflection FTIR spectroscopy. *EMBO J.* 14:5514–5523.

Taylor, H. P., S. J. Armstrong, and N. J. Dimmock. 1987. Quantitative relationships between an influenza virus and neutralizing antibody. *Virology.* 159:288–298.

Weber, T., G. Paesold, C. Galli, R. Mischler, G. Semenza, and J. Brunner. 1994. Evidence for H(+)-induced insertion of influenza hemagglutinin HA2 N-terminal segment into viral membrane. *J. Biol. Chem.* 269: 18353–18358.

Weissenhorn, W., A. Dessen, S. C. Harrison, J. J. Skehel, and D. C. Wiley. 1997. Atomic structure of the ectodomain from HIV-1 gp41. *Nature.* 387:426–430.

Wharton, S. A., L. J. Calder, R. W. Ruigrok, J. J. Skehel, D. A. Steinhauer, and D. C. Wiley. 1995. Electron microscopy of antibody complexes of influenza virus hemagglutinin in the fusion pH conformation. *EMBO J.* 14:240–246.

White, J. 1996. Membrane fusion: the influenza paradigm. *Cold Spring Harb. Symp. Quant. Biol.* 60:581–588.

Wiley, D. C., and J. J. Skehel. 1987. The structure and function of the hemagglutinin membrane glycoprotein of influenza virus. *Annu. Rev. Biochem.* 56:365–394.

Yu, Y. G., D. S. King, and Y. K. Shin. 1994. Insertion of a coiled-coil peptide from influenza virus hemagglutinin into membranes. *Science.* 266:274–276.

Zimmerberg, J., S. S. Vogel, and L. V. Chernomordik. 1993. Mechanisms of membrane fusion. *Annu. Rev. Biophys. Biomol. Struct.* 22:433–466.